

Supplementary Information

Au 4f spin-orbit coupling effects in supported gold nanoparticles

Sergey P. Chenakin ^{a,b} and Norbert Kruse ^{a,c,*}

^a *Chimie-Physique des Matériaux, Université Libre de Bruxelles (ULB), Bruxelles, Belgium*

^b *G.V. Kurdyumov Institute for Metal Physics NASU, Akad. Vernadsky Blvd. 36, 03680 Kiev, Ukraine*

^c *Voiland School of Chemical Engineering and Bioengineering, Washington State University, 155A Wegner Hall, Pullman, WA 99164-6515, USA*

* Corresponding author: E-mail: norbert.kruse@wsu.edu

1. Preparation of the samples

Au/TiO₂ catalysts were prepared by deposition–precipitation (DP) technique using different recipes and calcination conditions. In the first route, titanyl oxalate complex was precipitated through reaction of titanium tetraisopropoxide Ti(OC(CH₃)₃)₄ (>98%, Acros Organics) with a 10-fold excess of oxalic acid dihydrate (>99%, Acros Organics) in acetone (99.5%, Merck) followed by filtration and drying of the residue at 80°C overnight. Decomposition of the precipitate under 10% O₂ in Ar ambient at 560°C for 4 h yielded TiO₂. According to the X-ray diffraction analysis (XRD, RX Bruker with a graphite monochromator, Cu K α , 40 kV, 30 mA), the synthesized titania has an anatase structure (Fig. S1). Deposition–precipitation of Au nanoparticles (NP) on as-prepared TiO₂ was performed using an aqueous solution of HAuCl₄·3H₂O (99.9+%, Aldrich), the precipitating agent being 0.1 M NaOH (>98%, Aldrich) at pH \approx 7. After filtration and drying of the precipitate at 120°C overnight it was calcined in air at 400°C for 2 h. The Au/TiO₂ catalyst produced in this way is denoted as ‘GC1’. Its Brunauer–Emmet–Teller (BET) specific surface area was determined to be \sim 60 m²/g.

In the second route, titanyl oxalate complex was obtained by reacting Ti(OC(CH₃)₃)₄ with a 1.5-fold excess of H₂C₂O₄·2H₂O in acetone. To test the possible catalytic influence of Mg, TiOC₂O₄ was precipitated by adding MgNO₃·6H₂O (>98%, Riedel-de Haën) to the solution in amounts necessary for doping TiO₂ with 0.04 wt% Mg. The titanyl oxalate was decomposed under 10% O₂ in Ar ambient at 525°C for 4 h to form TiO₂ with anatase structure (XRD). To obtain a sodium-free catalyst, deposition–precipitation of Au on TiO₂ was performed from an aqueous solution of HAuCl₄ with another precipitating agent – urea CO(NH₂)₂ (>99%, Merck) at pH \approx 7. Care was also taken by using: (i) ultrapure water (Milli-Q); (ii) glass ware of quartz for the decomposition of titanyl oxalate and for catalytic tests; (iii) all other utensils of polypropylene washed with boric acid H₃BO₃ and rinsed several

times in ultra-pure water to eliminate traces of alkaline elements. The resulting Au/TiO₂ catalyst was calcined in the 10% O₂ in Ar ambient at 300°C for 2 h; its BET specific surface area was 100 m²/g. We denote this sample as ‘GC2’.

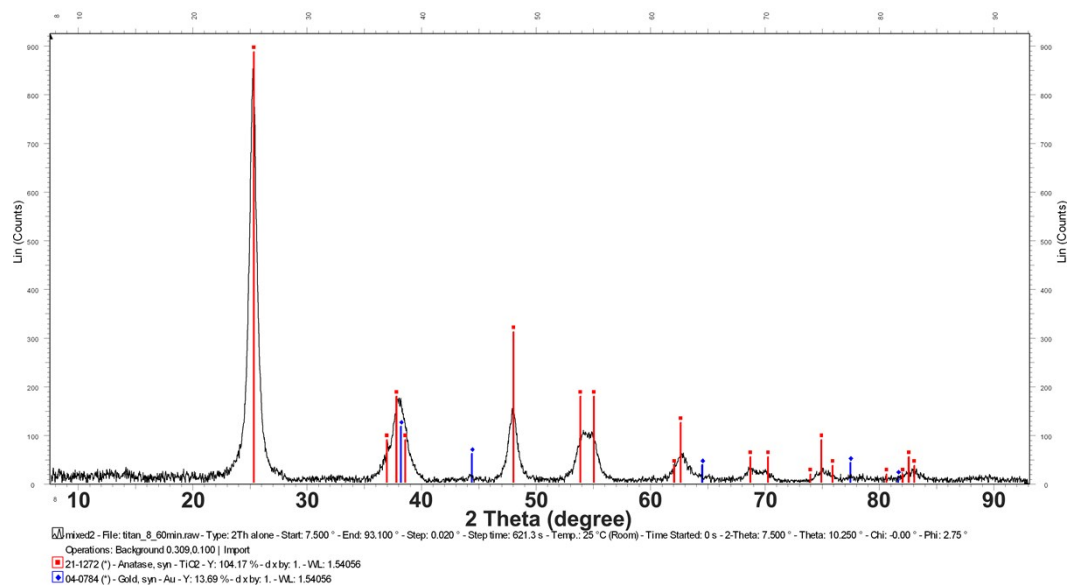


Fig. S1. XRD of the synthesized TiO₂ support corresponding to anatase structure.

Au/TiO₂ catalyst ‘GC3’ was synthesized in the same way as GC2, but in the absence of Mg(NO₃)₆H₂O. It was calcined in the 10% O₂ in Ar environment at 350°C for 2 h. As GC2, this catalyst was also purposely prepared in a sodium-free environment; its BET specific surface area was also ~ 100 m²/g.

In all the samples, GC1, GC2 and GC3, the amount of gold in the solution was adjusted to provide a loading of 1.5 wt% Au. The analysis of the catalyst GC2 by inductively coupled plasma atomic emission spectroscopy (ICP-AES; Perkin–Elmer Optima 3000XL) showed the Au content to be about 0.7 wt%, which is considerably lower than the nominal synthesis loading.

For comparison, the commercial Au/TiO₂ gold reference catalyst prepared by deposition–precipitation on commercial Degussa P25 TiO₂ and provided by the World Gold Council (WGC) (Lot No. #02-4, sample 23A) was also investigated. According to the certificate, the Au loading in the Au/TiO₂ WGC was 1.51 wt.% (ICP data) and the average Au particle diameter 3.8 ± 1.5 nm (TEM data).

All Au/TiO₂ catalysts were tested in CO oxidation at room temperature with a reactive gas mixture containing 2% CO + 2% O₂ (Ar balance) and exhibited variations in the initial activity, with the WGC and GC3 showing the highest CO-to-CO₂ conversion efficiency.

2. Transmission electron microscopy (TEM) analysis

The as-prepared Au/TiO₂ catalysts GC1, GC2 and GC3 were analyzed in an ultra-high resolution transmission electron microscope Philips CM20 (UltraTWIN STEM type) with a LaB₆ filament at 200 kV. The TEM micrographs of the catalysts are shown in Figs. S2, a–c.

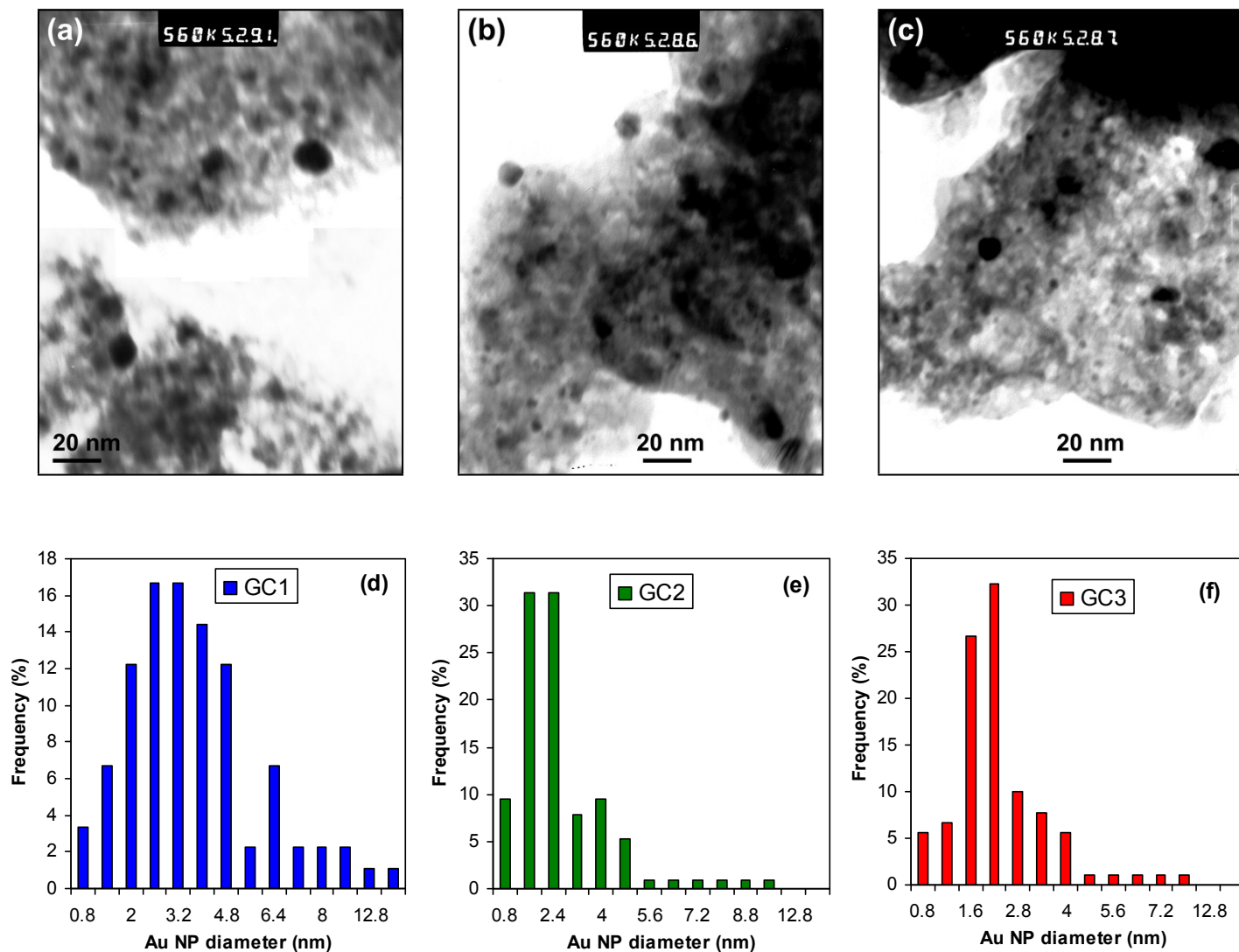


Fig. S2. TEM images (a–c) and Au particle size distributions (d–f) in the Au/TiO₂ catalysts GC1 (a, d), GC2 (b, e) and GC3 (c, f).

The particle size distribution was obtained by measuring 100-115 individual gold particles, and the average particle diameter was calculated by

$$d_{av} = \sum n_i d_i / \sum n_i,$$

where n_i is the number of particles of diameter d_i . The standard deviation was calculated using the formula:

$$\sigma = [\sum (d_i - d_{av})^2 / \sum n_i]^{1/2}.$$

Gold particle size distributions in the catalysts are plotted in Figs. S2, d–f. As can be seen in Fig. S2, d, catalyst GC1 is characterized by a wide bimodal particle size distribution ranging from subnanometer up to ca. 16 nm with an average particle diameter of 3.9 ± 1.9 nm. The most abundant gold particle size in this catalyst can be defined as 3.2 ± 0.3 nm. Catalyst GC2 displays an appreciably narrower Au particle size distribution, with only a small fraction of particles having a diameter > 5 nm (Fig. S2, e). The mean particle size of this catalyst is 2.6 ± 1.2 nm, and the most abundant particle diameter is 2.1 ± 0.1 nm. Catalyst GC3 demonstrates a similar narrow Au particle size distribution in the range up to 9.6 nm and a small fraction of large particles (Fig. S2, f), with the average particle diameter being 2.4 ± 1.1 nm and the most abundant diameter 2.0 ± 0.1 nm. These data show that the Au/TiO₂ samples prepared under sodium-free conditions are characterized by a smaller Au particle size and a significantly narrower particle size distribution.

3. XPS and ToF-SIMS analyses

Surface analysis of the catalysts by X-ray photoelectron spectroscopy (XPS) and time-of-flight secondary ion mass spectrometry (ToF-SIMS) was performed in a combined XPS–ToF-SIMS setup at a base pressure of $5.2 \cdot 10^{-10}$ mbar. For XPS-SIMS analyses, the powder of an Au/TiO₂ catalyst was pressed uniformly over an indium film on a flat sample holder to form a layer typically about 0.1 mm thick. Two samples could be placed together on the sample holder and sequentially analyzed under the same experimental conditions. Prior to analysis, the samples were outgassed for 120 h in a preparation chamber at a base pressure of $6 \cdot 10^{-10}$ mbar.

XP spectra were taken with a non-monochromatic Mg K_{α} radiation (15 kV \times 10 mA) and a hemispherical analyzer in the constant pass-energy mode at $E_p = 50$ eV with a 0.03 eV energy step. XPS analysis was performed for two to four samples of each catalyst. Mass spectra of emitted positive secondary ions were obtained with a pulsing beam of 5 keV Ar⁺ ions, using a reflectron analyzer. The spectra were taken in the mass range up to $m/e = 400$ with a mass resolution of $m/\Delta m = 1230$ at FWHM of $m/e = 51$.

In order to evaluate the surface composition of the samples and to determine the

atomic concentration of Au on the TiO₂ support, the areas under the XPS Au 4*f*, Ti 2*p*, O 1*s* and C 1*s* peaks and standard sensitivity factors were used. The Au surface atomic concentration in the Au/TiO₂ catalysts was found to vary in the range 0.26–0.73 at% (or 0.011–0.028 for Au/Ti atomic ratio) and tended to decrease in the series of the samples WGC > GC1 > GC2 ≈ GC3.

Figure S3 shows that binding energy of the Au4*f*_{7/2} photoelectrons in the Au/TiO₂ catalysts increases with decreasing Au concentration on the surface of TiO₂ support which corresponds also to a decrease in the TEM-derived average Au particle size in the series of catalysts WGC, GC1 > GC2, GC3. This dependence is similar to that obtained in a number of works in which the increase in the Au4*f*_{7/2} binding energy with decreasing (i) XPS-derived Au surface concentration [15*], (ii) Au surface coverage [4*, 5*, 7*] or (iii) Au film thickness [2*, 16*] was attributed to an Au particle size effect (the references [*] of these works are given in the main text).

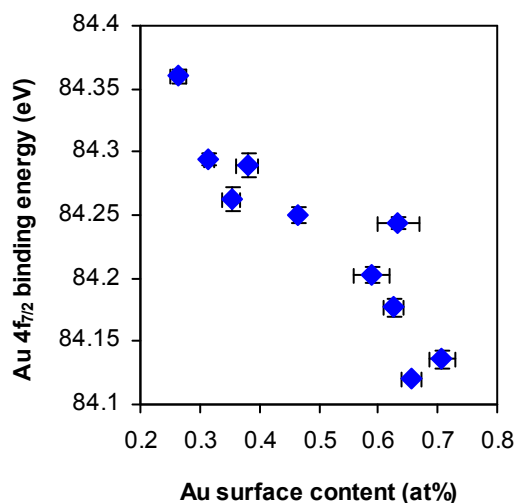


Fig. S3. The Au 4*f*_{7/2} binding energy as a function of Au concentration on the surface of TiO₂ support in various Au/TiO₂ catalysts GC1, GC2, GC3 and WGC.

Figure S4 shows the regions of mass spectra of secondary ions recorded for the GC1, GC2, GC3 and WGC Au/TiO₂ catalysts. All the spectra are reduced to the same intensity of the characteristic ⁴⁸Ti⁺ ion peak to enable a direct comparison of the normalized ion peak intensities M⁺/Ti⁺ in different samples. Note that SIMS, due to its extremely high sensitivity to alkali elements, allows their detection at a very low level. Indeed, as one can see, the GC1 (Fig. S4, a) and WGC (Fig. S4, d) samples demonstrate a rather intense emission of Na⁺ ions (in the given plots, the Na⁺ peak intensity is characteristic of the Na surface content in the

catalysts). On the contrary, the emission of Na^+ ions from GC2 and GC3 is very low, specifically about 36 times lower than that from GC1 and about 88 times lower than that in WGC, though the Na^+ signal in these catalysts could still be detected (Fig. S4, b, c). Thus, the obtained SIMS data confirm that the preparation recipe of GC2 and GC3 really ensured a significant diminution of the sodium content in the catalysts.

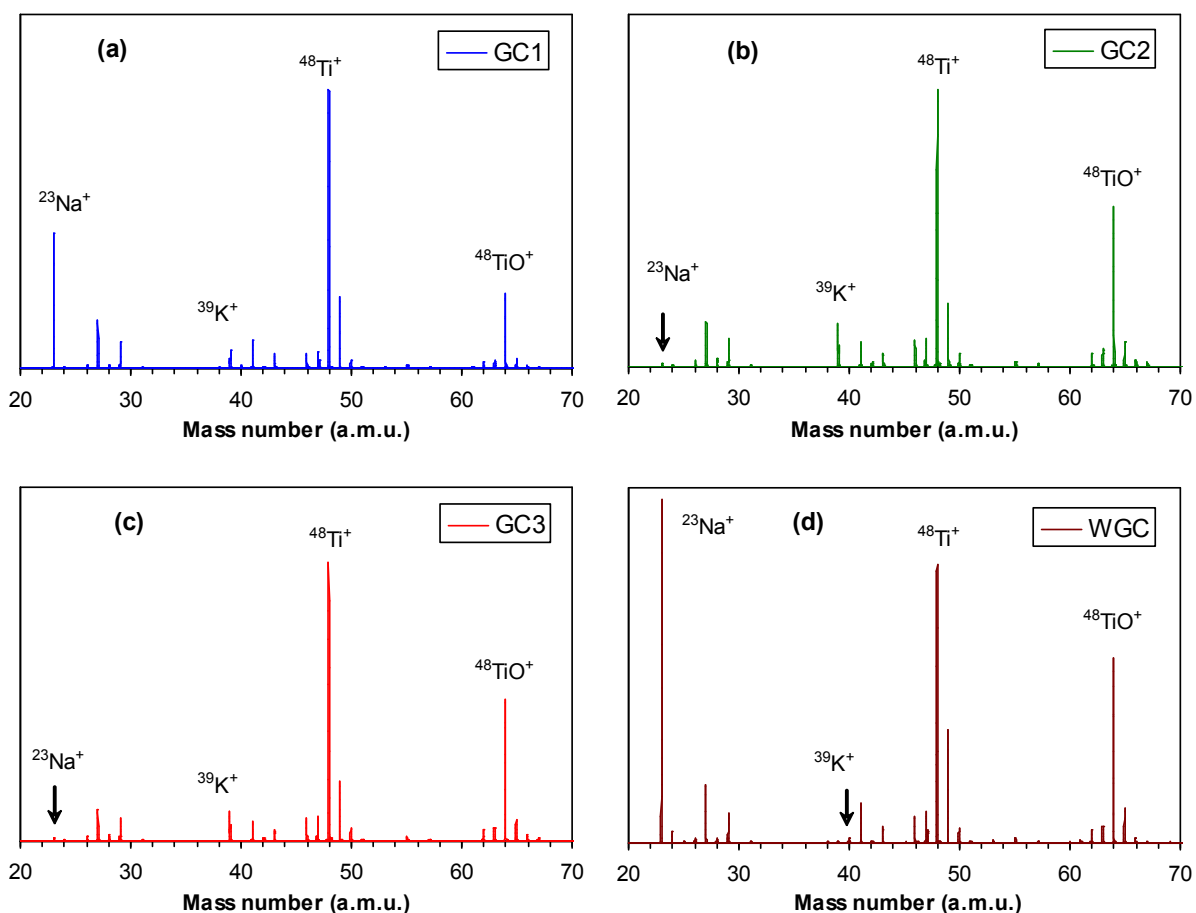


Fig. S4. Mass spectra of positive secondary ions emitted from the Au/TiO₂ catalysts GC1 (a), GC2 (b), GC3 (c) and WGC (d). All the spectra are reduced to the same intensity of the distinguished $^{48}\text{Ti}^+$ ion peak.

Unfortunately, the emission of Au^+ ions could not be detected because the Au surface concentration in all the Au/TiO₂ catalysts is very low (0.26–0.73 at%) and, in addition, because the gold has the lowest secondary ion yield (which is nearly 3 orders of magnitude lower than that for Ti in TiO₂) [1].

Interestingly, the normalized emission of sodium ions, Na^+/Ti^+ , from the catalysts appears to exhibit a direct correlation with the XPS-derived Au surface atomic content (or Au/Ti atomic ratio) (Fig. S5). This may indicate that Na^+ ions in the samples are located close

to Au nanoparticles. Accordingly, short-range electrostatic field Na–Au interaction or some electronic alterations might be envisaged.

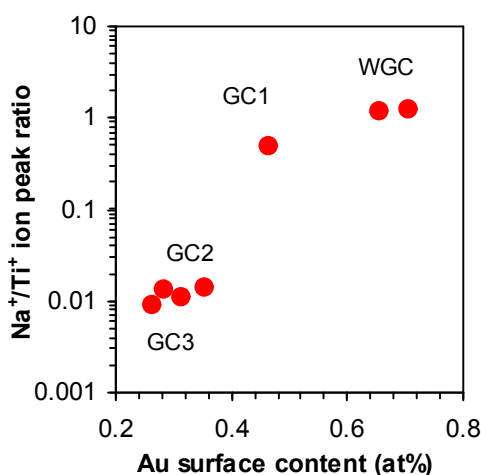


Fig. S5. The Na⁺/Ti⁺ ion peak ratio derived from SIMS measurements versus the XPS-derived Au surface content in the Au/TiO₂ catalysts GC1, GC2, GC3 and WGC.

However, the dependence of the Au4f_{7/2} binding energy on the Au surface content shown in Fig. S3, which reproduces the widely reported size effect and is supported by our TEM data, indicates that the presence of Na impurity does not noticeably affect the electronic structure of Au nanoparticles. On the other hand, an appreciably smaller average Au particle size in the sodium-free catalysts as compared to the catalysts with a high Na content implies that sodium might promote the nucleation and growth of the Au particles in the GC1 and WGC catalysts.

References

1. M.A. Vasil'ev, S.P. Chenakin and V.T. Cherepin, Determination of the relative secondary ion yields, *Zhurnal Analiticheskoy Khimii*, 1975, **30**, No. 3, 611 (in Russian).